ISTANBUL TECHNICAL UNIVERSITY ★ FACULTY OF AERONAUTICS AND ASTRONAUTICS

IMPLEMENTATION OF THE SUPERSONIC VORTEX LATTICE METHOD FOR WING CONFIGURATIONS

GRADUATION PROJECT

Kübra TEZCAN

Department of Aeronautical Engineering

Thesis Advisor: Prof. Dr. Melike NİKBAY

JULY, 2020

ISTANBUL TECHNICAL UNIVERSITY ★ FACULTY OF AERONAUTICS AND ASTRONAUTICS

IMPLEMENTATION OF THE SUPERSONIC VORTEX LATTICE METHOD FOR WING CONFIGURATIONS

GRADUATION PROJECT

Kübra TEZCAN
(110150601)

Thesis Advisor: Prof. Dr. Melike NİKBAY

JULY, 2020

Kübra Tezcan,student of ITU Faculty of Aeronautics and Astronauticsstudent ID **110150601**, successfully defended the **graduation** entitled "**IMPLEMENTATION OF THE SUPERSONIC VORTEX LATTICE METHOD FOR WING CONFIGURATIONS**", which she prepared after fulfilling the requirements specified in the associated legislations, before the jury whose signatures are below.

Thesis Advisor :	**Prof. Dr. Melike NİKBAY** İstanbul Technical University	.....
Jury Members :	**Prof. Dr. Mehmet ŞAHİN** İstanbul Technical University	.....
	Dr. Bülent TUTKUN İstanbul Technical University	.....

Date of Submission : 13 July 2020
Date of Defense : 21 July 2020

To my family,

FOREWORD

TABLE OF CONTENTS

Page

ABBREVIATIONS

LIST OF TABLES

LIST OF FIGURES

IMPLEMENTATION OF THE SUPERSONIC VORTEX LATTICE METHOD FOR WING CONFIGURATIONS

SUMMARY

1. INTRODUCTION

In computational fluid dynamics, there is always a need for a numerical method to calculate aerodynamic characteristics in the early design stages of aircraft, offering low computational costs and rapid results as well as approaching accurate results. The vortex lattice method (VLM) is a very easy and effective tool to meet these needs. The vortex lattice method is based on the potential flow theory, that is, the flow is considered ideal. In potential flow equations, the flow is accepted as irrotational and all boundary layer effects are neglected. In this method, any lifting surface is modelled by dividing it into panels on which vortices are placed, and the VLM use vortex singularity as the solution of the linearized potential equations, which is a type of Laplace equation. Pressure distribution is obtained by calculating the strenghts of the vortices placed on the lifting surfaces and this information is then used to calculate the aerodynamic coefficients and their derivatives. While simulating the lifting surfaces, a very thin structure is assumed by neglecting the thickness, besides this method gives more accurate results for low angle of attacks.

1.1 Purpose of Thesis

In this thesis, a module that can calculate aerodynamic characteristics will be developed based on the vortex lattice method developed by Carlson and Miller (1974) for supersonic flows $(1.2 < M < 5)$. Different wing configurations will be analyzed using this module. This method will be valid in the region where the flow is linear. In addition, as mentioned above, this method is based on potential flow theory, the flow is irrotational and accordingly, boundary layer effects will not be considered.

Firstly, in order to better understand the method, obtaining linearized potential flow equations will be explained and then vortex lattice method will be discussed. Then, the development of the module for supersonic speeds will be explained. Finally, validation of the analyzes for different wing types will be carried out so that the developed code will be tested.

1.2 Literature Review

Panel methods can be divided into two groups as lower and higher order. Terms called lower-order use singularity distributions with constant strength (Hess and Smith, 1962) on each panel, while terms called higher-order can use linear (Hess,1972) and quadratic (Morino and Kuo, 1974) singularity distributions or curved panels instead of constant.

Firstly, panel methods were developed for the analysis of incompressible and subsonic flows by using lower-order methods. Later, studies were made for supersonic flows and the first successful panel method for supersonic speeds was developed in the mid-1960s, again using lower-order methods (Erickson, 1990). To mention the vortex lattice method to be examined in this thesis, it is similar to the panel methods, and it is easier to use since it has a less complicated structure than panel methods. Because vortex lattice methods, like panel methods, are based on potential flow and derived from Laplace equations, vortex lattice methods have similar theories as panel methods.

Nae stated that the vortex lattice method is similar to the panel methods at the following points:

- singularities are placed on the lifting surface
- a system of linear equations is solved, to obtain singularity strengths

The vortex lattice method differs from the panel methods at the following points:

- no singularity distribution over the entire surface
- VLM neglects thickness, so it is valid for thin lifting surfaces
- boundary conditions are not applied to the actual surface, but to a mean surface (p.2, 2010)

The “Vortex Lattice” name was first used by Faulkner. He prepared a report titled "The Solution of Lifting Plane Problems by Vortex Lattice Theory" in 1947. In the 1950s, many studies were extensively performed to develop Faulkner's method. However, due to absence of computer capabilities at that time, the number of panels used in calculations was limited and a result of this, the accuracy of the results was questionable. The vortex lattice method was supposed to need computer capability. In the 1960s, four independent studies were carried out which were a continuation of

the Faulkner method and customized to electronic computers, and this studies belong to Rubbert (1964), Dulmovits (1964), Hedman (1966) and Belotserkovskii (1967) respectively. By the 1970s, NASA started a large-scale study of the vortex lattice method. By creating a universal standard, many new codes have been developed. The most recently developed and updated version by NASA in these studies is VLM4.997. Later, many codes were developed on this method. However, the code developed by NASA has become a standard with both accessibility and reliability.

2. POTENTIAL FLOW

2.1 Governing Equation

For objects having small angle of attack in uniform flow with high Reynolds number, if boundary layer effects can be neglected; we can say there is irrotational flow around these objects. The flow field under these conditions is called potential flow (Yukselen, 2007).

In this section, potential flow equation linearized by small perturbation method is developed. The equation is valid for steady, irrotational, compressible, subsonic flow or thin wings in supersonic flow at relatively small angles of attack.

Let define a velocity potential, $\phi = \phi(x, y)$ for steady, irrotational, isentropic flow such that

$$V = \nabla\phi \qquad (1.1)$$

$$u = \frac{\partial\phi}{\partial x}, \quad v = \frac{\partial\phi}{\partial y} \; and \; w = \frac{\partial\phi}{\partial z} \qquad (1.2)$$

Initially, to acquire an equation for ϕ as representation of continuity, momentum, and energy equations, the following procedures are fulfilled:

The continuity equation for three-dimensional flow is

$$\frac{\partial\rho}{\partial t} + \nabla.(\rho \boldsymbol{V}) = 0 \qquad (1.3)$$

Since $\frac{\partial\rho}{\partial t} = 0$ for steady flow, the continuity equation become

$$\nabla.(\rho \boldsymbol{V}) = 0 \quad (1.4)$$

$$\frac{\partial(\rho u)}{\partial x} + \frac{\partial(\rho v)}{\partial y} + \frac{\partial(\rho w)}{\partial z} = 0 \quad (1.5)$$

$$\frac{\partial u}{\partial x}+\frac{\partial v}{\partial y}+\frac{\partial w}{\partial z}=-\frac{1}{\rho}\left(u\frac{\partial \rho}{\partial x}+v\frac{\partial \rho}{\partial y}+w\frac{\partial \rho}{\partial z}\right) \qquad (1.6)$$

The differential form of momentum equation for three-dimensional flow is

$$\frac{\partial(\rho u)}{\partial t}+\nabla.(\rho u\boldsymbol{V})=-\frac{\partial P}{\partial x}+\rho f_x+(F_x)_{viscous} \quad (1.7a)$$
$$\frac{\partial(\rho v)}{\partial t}+\nabla.(\rho v\boldsymbol{V})=-\frac{\partial P}{\partial y}+\rho f_y+(F_y)_{viscous} \quad (1.7b)$$
$$\frac{\partial(\rho w)}{\partial t}+\nabla.(\rho w\boldsymbol{V})=-\frac{\partial P}{\partial z}+\rho f_z+(F_z)_{viscous} \quad (1.7c)$$

Since $\frac{\partial \rho}{\partial t}=0$ and $F_{viscous}=0$ for steady, inviscid flow with no body force $(f=0)$, the components of the momentum equation become

$$\nabla.(\rho u\boldsymbol{V})=-\frac{\partial P}{\partial x} \qquad \nabla.(\rho v\boldsymbol{V})=-\frac{\partial P}{\partial y} \qquad \nabla.(\rho w\boldsymbol{V})=-\frac{\partial P}{\partial z}$$
$$(1.8)$$

Then, the components of the momentum equation return to

$$u\frac{\partial u}{\partial x}+v\frac{\partial u}{\partial y}+w\frac{\partial u}{\partial z}=-\frac{1}{\rho}\frac{\partial P}{\partial x} \quad (1.9a)$$
$$u\frac{\partial v}{\partial x}+v\frac{\partial v}{\partial y}+w\frac{\partial v}{\partial z}=-\frac{1}{\rho}\frac{\partial P}{\partial y} \quad (1.9b)$$
$$u\frac{\partial w}{\partial x}+v\frac{\partial w}{\partial y}+w\frac{\partial w}{\partial z}=-\frac{1}{\rho}\frac{\partial P}{\partial z} \quad (1.9c)$$

The speed of sound is defined as the change in pressure with respect to the change in density for an isentropic process (Bertin, Cummings, 2009). Thus,

$$\frac{\partial P}{\partial \rho}=a^2 \quad (1.10)$$

Pressure terms in momentum equation, respectively return to

$$\frac{\partial P}{\partial x} = \frac{\partial P}{\partial \rho}\frac{\partial \rho}{\partial x} = a^2\frac{\partial \rho}{\partial x} \quad (1.11a)$$

$$\frac{\partial P}{\partial y} = \frac{\partial P}{\partial \rho}\frac{\partial \rho}{\partial y} = a^2\frac{\partial \rho}{\partial y} \quad (1.11b)$$

$$\frac{\partial P}{\partial z} = \frac{\partial P}{\partial \rho}\frac{\partial \rho}{\partial z} = a^2\frac{\partial \rho}{\partial z} \quad (1.11c)$$

Finally, the components of the momentum equation (1.9) become

$$u\frac{\partial u}{\partial x} + v\frac{\partial u}{\partial y} + w\frac{\partial u}{\partial z} = -\frac{a^2}{\rho}\frac{\partial \rho}{\partial x} \quad (1.12a)$$

$$u\frac{\partial v}{\partial x} + v\frac{\partial v}{\partial y} + w\frac{\partial v}{\partial z} = -\frac{a^2}{\rho}\frac{\partial \rho}{\partial y} \quad (1.12b)$$

$$u\frac{\partial w}{\partial x} + v\frac{\partial w}{\partial y} + w\frac{\partial w}{\partial z} = -\frac{a^2}{\rho}\frac{\partial \rho}{\partial z} \quad (1.12c)$$

If the components of the momentum equation (1.12) are multiplied by u, v, and w respectively, and then the components are summed,

$$u^2\frac{\partial u}{\partial x} + v^2\frac{\partial v}{\partial y} + w^2\frac{\partial w}{\partial z} + uv\left(\frac{\partial u}{\partial y} + \frac{\partial v}{\partial x}\right) + uw\left(\frac{\partial u}{\partial z} + \frac{\partial w}{\partial x}\right) + vw\left(\frac{\partial v}{\partial z} + \frac{\partial w}{\partial y}\right) = -\frac{a^2}{\rho}\left(u\frac{\partial \rho}{\partial x} + v\frac{\partial \rho}{\partial y} + w\frac{\partial \rho}{\partial z}\right) \quad (1.13)$$

Equation (1.13) and continuity equation are combined, density terms is eliminated from the equation (1.13), and so a useful equation based on only velocity components and sound velocity is obtained.

$$\left(1 - \frac{u^2}{a^2}\right)\frac{\partial u}{\partial x} + \left(1 - \frac{v^2}{a^2}\right)\frac{\partial v}{\partial y} + \left(1 - \frac{w^2}{a^2}\right)\frac{\partial w}{\partial z} - 2\frac{uv}{a^2}\frac{\partial u}{\partial y} - 2\frac{vw}{a^2}\frac{\partial v}{\partial z} - 2\frac{wu}{a^2}\frac{\partial w}{\partial x} = 0 \quad (1.14a)$$

Recall that, in the beginning, we introduce a velocity potential such that $u = \frac{\partial \phi}{\partial x}$, $v = \frac{\partial \phi}{\partial y}$ and $w = \frac{\partial \phi}{\partial z}$. By substituting velocity potential into equation, equation $(1.14a)$ returns to

$$\left(1 - \frac{\phi_x{}^2}{a^2}\right)\phi_{xx} + \left(1 - \frac{\phi_y{}^2}{a^2}\right)\phi_{yy} + \left(1 - \frac{\phi_z{}^2}{a^2}\right)\phi_{xx} - 2\frac{\phi_x\phi_y}{a^2}\phi_{xx} - 2\frac{\phi_y\phi_z}{a^2}\phi_{yy} - 2\frac{\phi_z\phi_x}{a^2}\phi_{zz} = 0 \qquad (1.14b)$$

which is the full potential equation. As can be seen above, this full potential equation is nonlinear, as a result of this, it is highly difficult to solve this equation both analytically and numerically. Consequently, the equation needs to be simplified to acquire analytic and numerical solutions. This simplification is made by considering the flow around the body, as a superposition of the uniform-parallel flow and the small perturbations flow created by the body. Thus, it is possible to linearize the equation with small perturbation method and solve potential flow equations (Yukselen, 2007).

Accordingly, as seen in the figure, at a point around a thin object in the uniform-parallel flow, the flow velocity can be expressed by the superposition of the free-stream velocity (a constant) and the perturbation velocity created by the object, respectively, $u', v', and\ w'$.

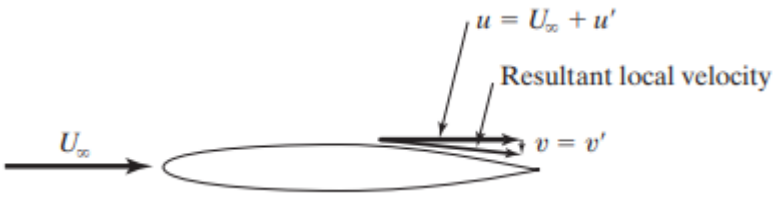

Figure 1.1 *Velocity components for compressible flow past a thin airfoil at a small angle of attack.*

$$u = U_\infty + u'$$
$$v = v'$$
$$w = w'$$

When free-stream velocity is compared with the perturbation velocities, it can be considered the perturbation velocities are smaller in magnitude $(u',\ v',\ w' \ll U_\infty)$. Then, equation $(1.14a)$ above becomes

$$\left(1-\frac{u^2}{a^2}\right)\frac{\partial u}{\partial x}+\frac{\partial v}{\partial y}+\frac{\partial w}{\partial z}=0 \qquad (1.15)$$

where $\frac{u}{a}$ is equal to the local Mach number. Since $\frac{a_1^2}{\gamma-1}+\frac{u_1^2}{2}=\frac{a_2^2}{\gamma-1}+\frac{u_1^2}{2}=\frac{a_0^2}{\gamma-1}$ from energy equation for steady, adiabatic, inviscid flow, local speed of sound can be determined as (Bertin, Cummings, 2009)

$$\frac{a^2}{\gamma-1}+\frac{u^2+v^2+w^2}{2}=\frac{a_\infty^2}{\gamma-1}+\frac{U_\infty^2}{2}=\frac{a_0^2}{\gamma-1} \qquad (1.16)$$

$$\frac{a^2}{a_\infty^2}=1-\frac{\gamma-1}{2}\left(\frac{u^2+v^2+w^2}{U_\infty^2}-1\right)M_\infty^2 \qquad (1.17)$$

Since it is concentrated only on small perturbations, that relationship (1.17) can be generated with the binominal theorem:

$$\frac{a_\infty^2}{a^2}=1+\frac{\gamma-1}{2}M_\infty^2\left(2\frac{u'}{U_\infty}+\frac{u'^2+v'^2+w'^2}{U_\infty^2}\right) \qquad (1.18)$$

To simply equation (1.15), $\left(1-\frac{u^2}{a^2}\right)$ term is rearranged as

$$\begin{aligned}1-\frac{u^2}{a^2}&=1-\frac{(U_\infty+u')^2}{a^2}\frac{U_\infty^2}{U_\infty^2}\frac{a_\infty^2}{a_\infty^2}\\&=1-\frac{U_\infty^2+2u'U_\infty+u'^2}{U_\infty^2}M_\infty^2\frac{a_\infty^2}{a^2}\end{aligned} \qquad (1.19)$$

Then, equation (1.18) is substituted into equation (1.19) by neglecting the higher-order terms

$$1-\frac{u^2}{a^2}=1-M_\infty^2\left[1+\frac{2u'}{U_\infty}\left(1+\frac{\gamma-1}{2}M_\infty^2\right)\right] \qquad (1.20)$$

By using equation (1.20), equation (1.15) is rewritten as:

$$(1-M_\infty^2)\frac{\partial u}{\partial x}+\frac{\partial v}{\partial y}+\frac{\partial w}{\partial z}=M_\infty^2\left(1+\frac{\gamma-1}{2}M_\infty^2\right)\frac{2u'}{U_\infty}\frac{\partial u}{\partial x} \qquad (1.21)$$

This equation can be rewritten in terms of the perturbation velocities as:

$$(1-M_\infty^2)\frac{\partial u'}{\partial x}+\frac{\partial v'}{\partial y}+\frac{\partial w'}{\partial z}=\frac{2}{U_\infty}\left(1+\frac{\gamma-1}{2}M_\infty^2\right)M_\infty^2u'\frac{\partial u'}{\partial x} \qquad (1.22)$$

Recall that the perturbation velocity components are so small in magnitude. Since, the perturbation velocity components with their derivatives are also small, we often neglect the right-hand side term of the above equation (1.22) by making the assumptions:

$$M_\infty^2\left(\frac{u'}{U_\infty}\right)^2\ll 1 \quad M_\infty^2\left(\frac{v'}{U_\infty}\right)^2\ll 1 \quad M_\infty^2\left(\frac{w'}{U_\infty}\right)^2\ll 1$$

$$M_\infty^2\left(\frac{u'v'}{U_\infty}\right)\ll 1 \quad M_\infty^2\left(\frac{u'w'}{U_\infty}\right)\ll 1 \quad M_\infty^2\left(\frac{v'w'}{U_\infty}\right)\ll 1$$

$$\frac{M_\infty^2}{|1-M_\infty^2|}\left(\frac{u'}{U_\infty}\right)\ll 1 \quad M_\infty^2\left(\frac{v'}{U_\infty}\right)\ll 1 \quad M_\infty^2\left(\frac{w'}{U_\infty}\right)\ll 1$$

Under the all assumptions, we can finally reach the target, and acquire the linearized equation:

$$(1-M_\infty^2)\frac{\partial u'}{\partial x}+\frac{\partial v'}{\partial y}+\frac{\partial w'}{\partial z}=0 \qquad (1.23)$$

If we introduce a potential function for perturbation velocities such that $u = \frac{\partial \phi'}{\partial x}$, $v = \frac{\partial \phi'}{\partial y}$ and $w = \frac{\partial \phi'}{\partial z}$, equation above becomes

$$(1 - M_\infty^2)\phi'_{xx} + \phi'_{yy} + \phi'_{zz} = 0 \qquad (1.24)$$

which is the linearized velocity potential equation for completely subsonic, compressible flow. Also, note that it is a linear, second-order partial differential equation of the elliptic type.

If we rewrite equation (1.24) in standard form (to have a positive factor for the ϕ_{xx} term) :

$$(M_\infty^2 - 1)\phi_{xx} - \phi_{yy} - \phi_{zz} = 0 \qquad (1.25)$$

where ϕ is the perturbation potential. This equation is the linearized velocity potential equation for compressible, supersonic flow in the range $1.2 \leq M_\infty \leq 5$. Also, note that it is a linear, second-order partial differential equation of the hyperbolic type.

2.2 Elementary Velocity Potential Equations

In the previous section, we introduced the governing equation linearized with assumption of small perturbations for compressible, irrotational flow. Linearized potential flow equations allow complex problems to be solved by simplifying them. To obtain a solution, a complicated flow can be represent by combining several elementary flows (i.e, source, doublet, horseshoe vortex).

The elementary potential flow equations given by Lomax et al. (1951) and used in supersonic cases are summarized in Table 1.2 as follows:

	Source	Doublet	Vortex
Elementary Potential Flow	$\phi_s = -\frac{Q}{r_c}$	$\phi_d = +\frac{Qz\beta^2}{r_c^3}$	$\phi_s = -\frac{Qzv_c}{r_c}$

Table 1.2 *The elementary supersonic source, the doublet, and the horseshoe vortex potentials given by Lomax et al. (1951)*

In the equations, Q is the strength of the singularity and the other terms are as follows:

$$\beta^2 = M_\infty^2 - 1$$

$$v_c = \frac{x - x_1}{(y - y_1)^2 + z^2}$$

$$r_c = \{(x - x_1)^2 - \beta^2[(y - y_1)^2 + z^2]\}^{0.5}$$

Also, note that the point (x_1, y_1, z_1) is the location of the singularity.

3. VORTEX LATTICE METHOD

3.1 Purpose

In this section, before explaining the method of vortex lattice method which is an implementation of supersonic flows, basic concepts of vortex lattice method will be mentioned.

The Vortex Lattice Method is a numerical method built on potential flow theory. This method is created on the idea of using vortex singularity as the solution of the linearized potential equations obtained above, which is a type of Laplace equation. Like potential flow theory, the VLM also assumes there is no viscous effect in flow, in other words, an ideal flow assumption is made. By using this method, high accuracy analyzes can be performed for thin objects with a small angle of attack.

During the analysis in this method, any lifting surfaces, such as wing, is divided into the desired number of panels. A horseshoe vortex is placed on each panel and the strength of each horseshoe vortices are found by considering the geometry and boundary condition factors.

In this section, before starting the methodology used, the assumptions made on the basis of this method will be mentioned and then the method will be discussed exactly.

3.2 Assumptions

The assumptions made on the basis of generating the vortex lattice method are listed below.

- The flow field is inviscid, irrotational, incompressible or compressible with small disturbance.
- The lifting surfaces of arbitrary profile are assumed to be thin, and the impact of thickness is negligible.
- VLM is applicable to planforms having small angle of attack. Since small angle approximation is made, this method works very well for lifting surfaces with small angle of attack.

3.3 Methodology

As previosly mentioned, a lifting surface is modelled as a number of quadrilateral panels on which vortices are placed. The specific form of vortices used in this method is horseshoe vortex. A horseshoe vortex system consists of the bound vortex system and two trailing vortex system [fig.3.3.1].

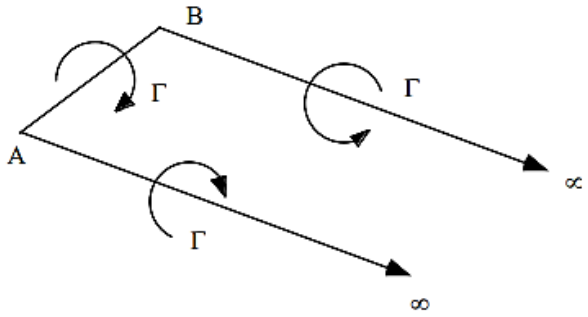

Figure 3.3.1 *The horseshoe vortex system*

In VLM, a bound vortex is placed in quarter (¼) chord position of each panel, while two trailing vortex lines alligned parallel to aircraft axis extend ends of each panel to infinity. In other words, a horseshoe vortex comes from infinity to end of the panel, and advance through the ¼ chord position of the panel, and finally go back to infinity from the other end of the panel [fig. 3.3.2].

The important parameter to be calculated is required vortex strenght of each panel. In here, since strength of the each horseshoe vortex is an unknown of the problem, the boundary condition on the surface is used to solve these unknowns. Then, after the necessary boundary conditions are met, a solution for calculating the vortex strenght can be developed.

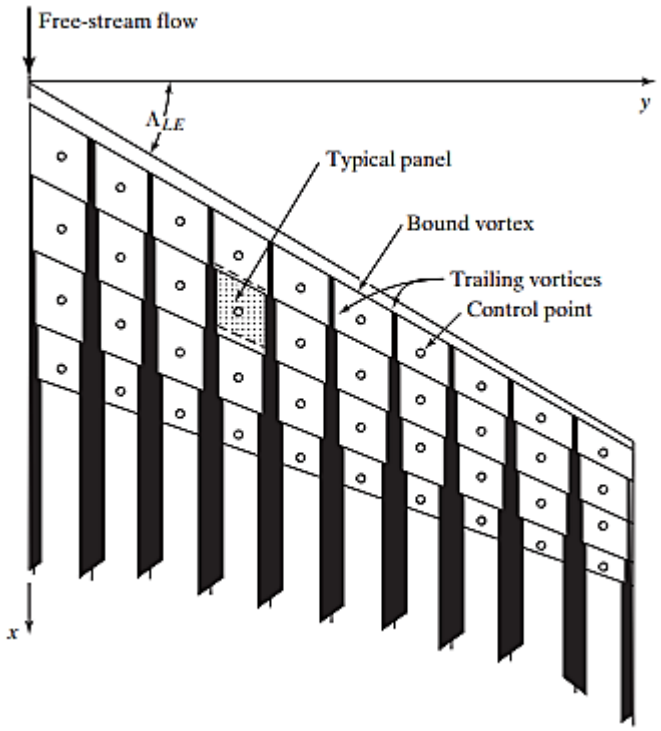

Figure 3.3.2 *Panels and horseshoe vortices for a swept-wing planform in the VLM.* [Bertin and Cummings, 2013]

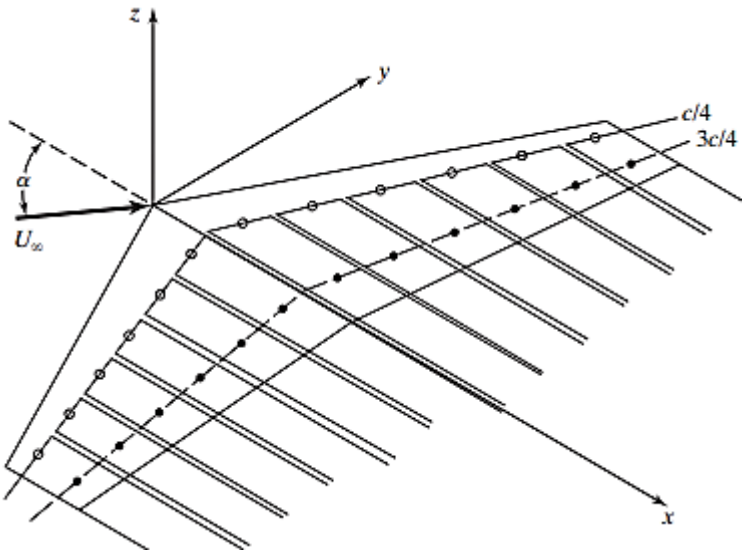

Figure 3.3.3 *Locations of bound vortices and control points for swept-wing. While the filled circles represent control points, the others represent the vortices* [Bertin and Cummings, 2013].

3.4 Boundary Condition and Solution Method

In this section, boundary conditions can be introduced firstly as follows:

- First condition that must be applied is Kutta condition. The flow must leave the object properly.
- Secondly, magnitude of velocity vectors in normal direction to the surface should be zero.

First condition is achieved by locating each control point in the middle of the three-quarters (¾) position of each panel [fig. 3.3.3]. Thus, each control point is positioned at the three-quarter (¾) chord position of the panel, while each bound vortex corresponds to one-quarter position. Mason stated that this placement is known as the "$1/4$ - $3/4$ $rule$". This is not a law, there are many mathematical studies that determine more precise vortex and control point locations, for example Lan (1974). However, as the accuracy of "$1/4$ - $3/4$ $rule$" has been proved in many studies, it has become the basic rule (1995). The derivation of this rule will not be studied here. For detailed information, reference 6 can be examined.

Second condition can be mathematically described as

$$\vec{V}.\hat{n} = 0 \qquad (2.1.1)$$

There are two factors that contribute to the velocity vector in normal direction on the surfaces. One of them is velocity component caused by freestream and the other is the induced velocities created by all horseshoe vortices. To achieve second boundary condition, the sum of these two components must be zero. As the induced velocity is a function of all vortex strenghts, a set of lineer equations can be developed to find vortex strengths by applying second boundary condition.

The main purpose is to equalize the normal velocity vector obtained at the control points to zero. Since the normal velocity is consist of normal freestream velocity component and induced velocity component, above equation $(2.1.1)$ can be written as

$$\vec{V}.\hat{n} = U_\infty sin\alpha + w_i = 0 \qquad (2.1.2)$$

where U_∞ is the freestream velocity, α is the angle of attack, and w_i is the induced velocity component.

Let define the induced velocity at the mth control point by horseshoe vortex locating in nth panel as

$$\overrightarrow{V_{m,n}} = \overrightarrow{C_{m,n}}\,\Gamma_n \qquad (2.1.3)$$

where $\overrightarrow{C_{m,n}}$ is influence coefficient for the vortex effect locating in n at the mth control point . It changes depending on both the geometry of the nth vortex and distance between the control point of the mth panel and the nth horseshoe vortex.

As mentioned earlier, we have linear governing equation. Thus, if we have N panels and, accordingly, N vortices, the total induced velocity at the mth control point can be found as the sum of the individually induced velocity by all these N vortices on panels.

$$\overrightarrow{V_m} = \sum_{n=1}^{N} \overrightarrow{C_{m,n}}\,\Gamma_n \qquad (2.1.4)$$

Since we have N control point, we will have N equation like above. So induced velocity component w_i in equation $(2.1.2)$ can be described as sum of the all N induced velocity equation:

$$w_i = \sum_{n=1}^{N} \overrightarrow{C_{m,n}}\,\Gamma_n \qquad (2.1.5)$$

Thus, equation $(2.1.2)$ becomes

$$\vec{V}.\hat{n} = U_\infty sin\alpha + \sum_{n=1}^{N} \overrightarrow{C_{m,n}}\,\Gamma_n = 0 \qquad (2.1.6)$$

$$\sum_{n=1}^{N} \overrightarrow{C_{m,n}}\,\Gamma_n = -U_\infty sin\alpha \qquad (2.1.7)$$

Assuming small angles of attack, $sin\alpha \approx \alpha$ radians,

$$\sum_{n=1}^{N} \overrightarrow{C_{m,n}}\,\Gamma_n = -U_\infty \alpha \qquad (2.1.8)$$

This equation can be demonstrated with system of equations like that

$$\begin{bmatrix} C_{11} & \cdots & C_{1N} \\ \vdots & \ddots & \vdots \\ C_{N1} & \cdots & C_{NN} \end{bmatrix} \begin{bmatrix} \Gamma_1 \\ \Gamma_2 \\ \vdots \\ \Gamma_n \end{bmatrix} = \begin{bmatrix} -U_\infty \alpha \\ -U_\infty \alpha \\ \vdots \\ -U_\infty \alpha \end{bmatrix} \qquad (2.1.9)$$

Consequently, the strength of each horseshoe vortex (Γ_n) can be obtained by solving this linear system of equations $(2.1.9)$. To find influence coefficient matrix of C_{mn}, Biot-Savart rule can be used.

3.5 Velocity Induced by a Horseshoe Vortex

The Biot-Savart law is a method used to find the velocities induced by each horseshoe vortex at each control point. This section explaining Biot-Savart rule is prepared by reference to Bertin's book.

Let define a finite-length vortex segment AB [fig.3.5.1] having strength Γ_n and a length of dl. The velocity induced by this vortex is

$$\overrightarrow{dV} = \frac{\Gamma_n(\vec{dl} \times \vec{r})}{4\pi r^3} \qquad (2.2.1)$$

According to figure 2.2.2.1, the magnitude of the velocity induced is

$$dV = \frac{\Gamma_n sin\theta\ dl}{4\pi r^2} \qquad (2.2.2)$$

Let say C is any point in space and normal distance between vortex segment AB and C is r_p. The magnitude of the induced velocity can be found by integrating between A and B:

$$V = \frac{\Gamma_n}{4\pi r_p} \int_{\theta_1}^{\theta_2} sin\theta\ d\theta = \frac{\Gamma_n}{4\pi r_p} (cos\theta_1 - cos\theta_2) \qquad (2.2.3)$$

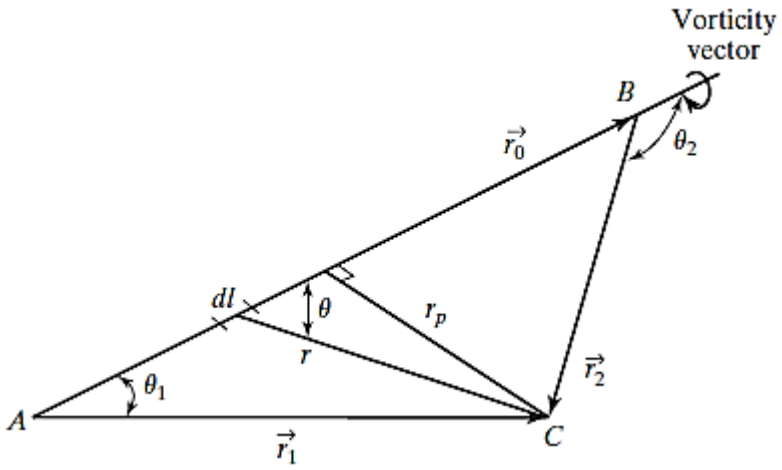

Figure 3.5.1 *Nomenclature for calculating the velocity induced by a finite-length vortex segment* [Bertin and Cummings, 2013].

Let $\vec{r_0}$, $\vec{r_1}$, and $\vec{r_2}$ in figure 2.2.2.1 represent respectively the vectors $\overrightarrow{AB}, \overrightarrow{AC}, \text{ and } \overrightarrow{BC}$. Then,

$$r_p = \frac{|\vec{r_1} \times \vec{r_2}|}{r_0} \qquad cos\theta_1 = \frac{\vec{r_0} \cdot \vec{r_1}}{r_0 r_1} \qquad cos\theta_2 = \frac{\vec{r_0} \cdot \vec{r_2}}{r_0 r_2}$$

These notations are substituted into equation (2.2.3):

$$\vec{V} = \frac{\Gamma_n}{4\pi} \frac{\vec{r_1} \times \vec{r_2}}{|\vec{r_1} \times \vec{r_2}|^2} \left[\vec{r_0} \cdot \left(\frac{\vec{r_1}}{r_1} - \frac{\vec{r_2}}{r_2}\right)\right] \qquad (2.2.4)$$

Finally, it is reached to the basic formulation used to calculate the velocities induced by vortices in the VLM.

As mentioned previously, a typical horseshoe vortex include three segments, and these are a bound vortex and two trailing vortices. The resultant velocity induced by a horseshoe vortex is found as sum of the three segments. In this study, velocity induced by bound vortex is only examined but the ways of obtaining total induced velocity by summing all three segments are not examined. However, for additional information, Bertin's book can be reviewed as reference.

3.6 Kutta-Joukovski Theorem

The strength of vortices has been found after the calculations mentioned in previous sections have been carried out. With these vortex strengths, the lift produced by any lifting surface can be obtained easily thanks to the Kutta-Joukovski's theorem.
By using the Kutta-Joukovski law, the lift produced on a particular panel is

$$l_i = \rho_\infty U_\infty \, \Gamma_i$$

Total lift of a lifting surface can be obtained by summing the all panel lift components:

$$L = \int_{i=1}^{N} l_i = \int_{i=1}^{N} \rho_\infty U_\infty \, \Gamma_i$$

4. SUPERSONIC VORTEX LATTICE METHOD ANALYSIS

In this thesis, a numerical application of the vortex lattice method will be developed for supersonic flow. Whereas there are many detailed numerical applications to several wing platforms, a supersonic VLM module will be developed with reference to the study of Carlson and Miller in 1974.

Before explaining the supersonic vortex method developed by Carlson and Miller, Mach cone and Mach angle concepts specific to supersonic flows will be discussed in order to understand the method more easily

4.1 Mach Cone and Mach Angle

“The speed of sound is defined as the rate at which infinitesimal disturbances are propagated from their source into an undisturbed medium. These disturbances can be thought of as small pressure pulses generated at a point and propagated in all directions" (Anderson, 2016).

The sound wave appearance of an object moving at subsonic speeds is as seen in figure 4.1.1. When the speed of the object reaches the speed of sound, the sound wave appearance changes as figure 4.1.2.

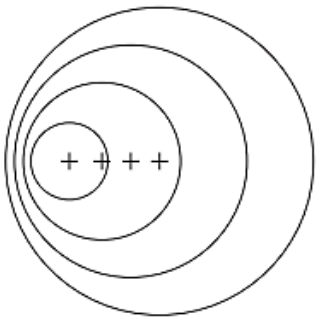

Figure 4.1.1 *Wave pattern at subsonic speeds.*

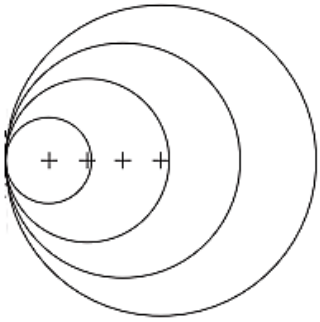

Figure 4.1.2 *Wave pattern at sonic speed.*

[Bertin and Cummings, 2013]

If the object accelerates more and moves at supersonic speeds, the sound wave appearance of the object is as follows.

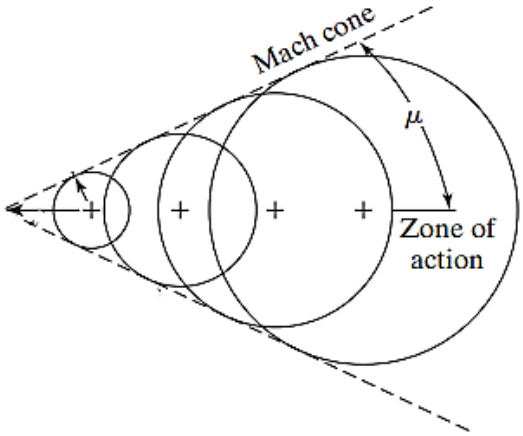

Figure 4.1.3 *Wave pattern at supersonic speeds.* [Bertin and Cummings, 2013]

As seen in the figures, as the object accelerates and approaches the supersonic velocity, the sound waves get closer to each other. Bertin says that waves approaching each other create a conical envelope, defined as the Mach cone. The area created by this mach cone is defined as the zone of action, and any disturbance effect exists only in this zone (2013). The effect of this situation on supersonic VLM analysis is that the interaction of some panels will be disrupted and discontinuity will occur.

Also, Mach angle μ which is the half angle of the Mach cone in figure 4.1.3 can be found directly depending on Mach number as following:

$$\mu = sin^{-1}\left(\frac{1}{M}\right)$$

4.2 Carlson and Miller Method

Carlson and Miller introduced a different numerical application to the supersonic vortex method in 1974. Any thin wing or lifting surface can be analyzed with this method.

In addition, following the adoption of the supersonic linearized theory, the thickness of this wing is assumed to be negligible, and it is consequently accepted that the wing lies in the plane $z = 0$ (Bertin,Cummings, 2013).

Carlson and Miller says that the differential pressure coefficient at any point (x, y) of a surface with a vortex distribution can be found as following equation:

$$\Delta C_p(x,y) = -\frac{4}{\beta}\frac{\partial z_c(x,y)}{\partial x} + \frac{1}{\pi}\iint R(x-x_1, y-y_1)\Delta C_p(x_1,y_1)d\beta y_1 dx_1 \qquad (4.1)$$

where $z_c(x,y)$ represents z coordinate of camber line and R is the influence function (Bertin, 2013). R and β are obtained as respectively:

$$R(x-x_1, y-y_1) = \frac{x-x_1}{\beta^2(y-y_1)^2[(x-x_1)^2-\beta^2(y-y_1)^2]^{0.5}} \qquad (4.2)$$

$$\beta = \sqrt{M_\infty^2 - 1} \qquad (4.3)$$

The integral in the equation (4.1), on the other hand, represents the effect of the continuous horseshoe vortices on the wing divided into panels. Besides, the integration region (S) emanating from the point of of influence (x, y) can be shown in figure 4.2.1. It can be said for a wing surface that the integration area are between the leading edge and the forecone Mach lines emanating from field point (x, y).

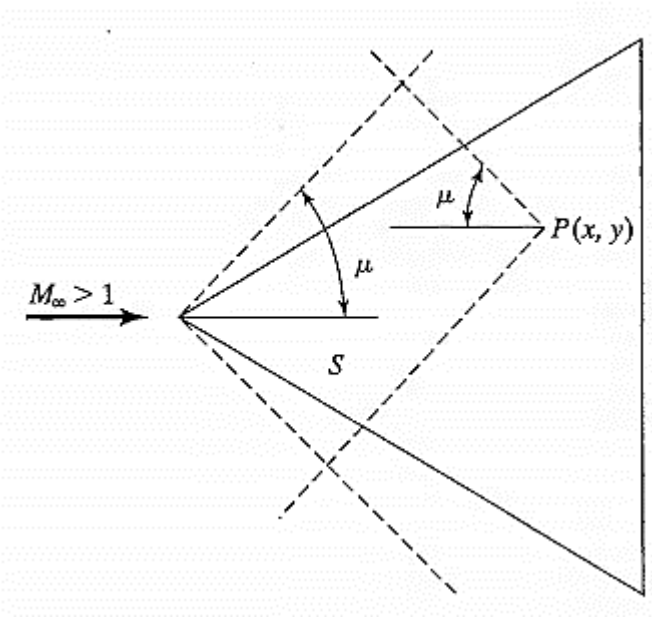

Figure 4.2.1 *S is the region of integration for the supersonic vortex lattice method.*

[Bertin and Cummings, 2013]

To be able to express the integral equation (4.1) in the form of an algebraic sum, a coordinate system change must firstly be made. In this way, it will be possible to express the integration region with panels. Therefore, the Cartesian coordinate system indicated in figure 4.2.2 is converted to the grid system in figure 4.2.3. The initial integration area S now consists of a series of grid elements that approximate the previous integration region.

Thus, using a grid elements system, a numerical method can be developed to calculate the pressure distribution. In the grid system [fig. 4.2.2], whereas L and N numbers define the spaces between the panels and are used instead of $d\beta y_1$ and dx_1 in the integral equation, $L^* and\ N^*$ represent the element of the field point $(x, \beta y)$. It should also be noted that L and N can only have integer values and the Mach cone half-angle will always be $45°$ in the grid coordinate system.

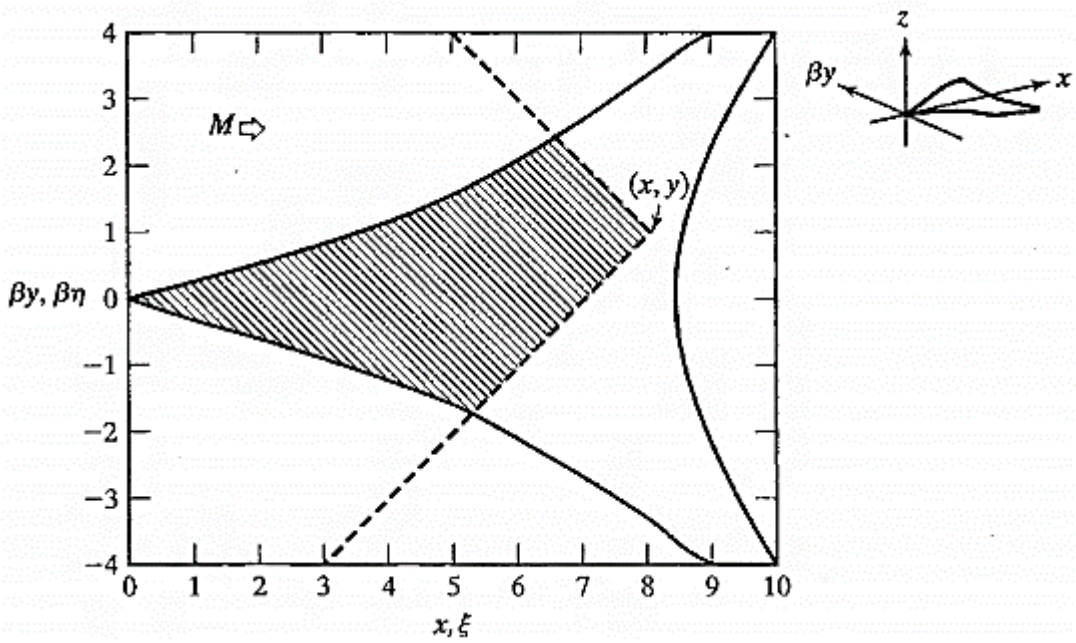

Figure 4.2.2 *Cartesian coordinate systems for the supersonic vortex lattice method*
[Bertin and Cummings, 2013]

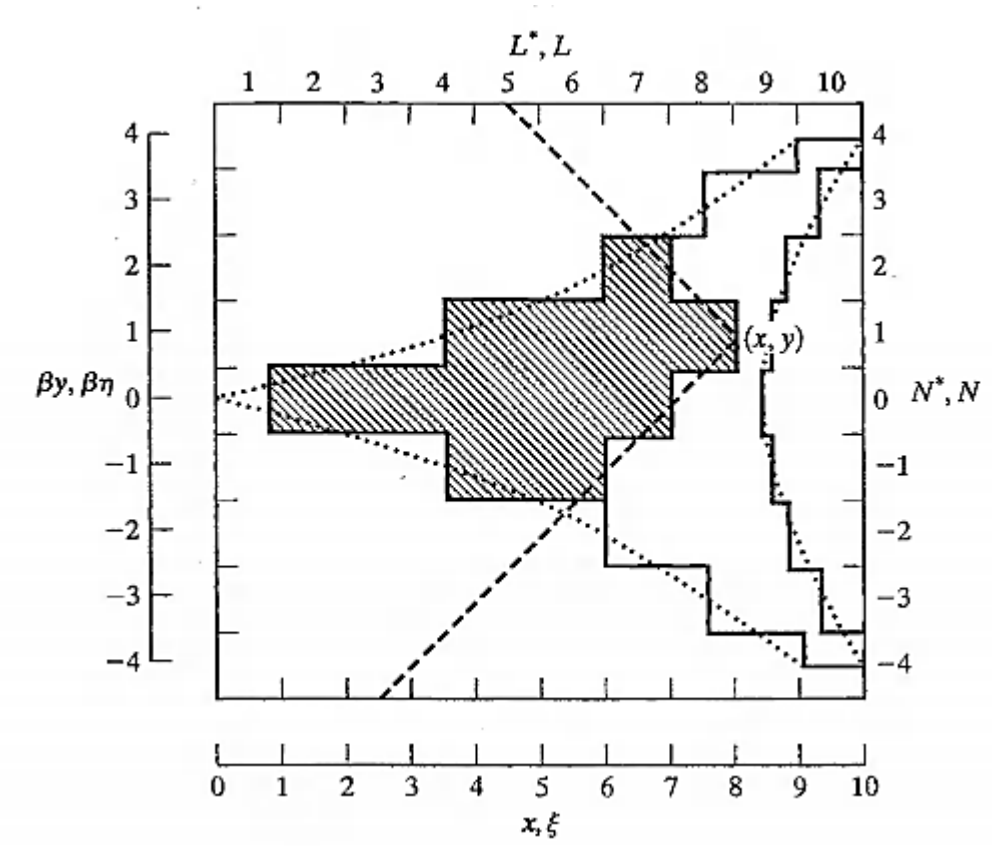

Figure 4.2.3 *Grid system used in numerical solution* [Bertin and Cummings, 2013].

After all coordinate system changes and summation approaches, the equation (4.1) becomes

$$\Delta C_p(L^*,N^*) = -\frac{4}{\beta}\frac{\partial z_c(L^*,N^*)}{\partial x} + \frac{1}{\pi}\sum_{N_{min}}^{N_{max}}\sum_{L_{LE}}^{L^*-|N^*-N|} \bar{R}\,(L^*-L,N^*-N)A(L,N)B(L,N)C(L,N)\Delta C_p(L,N) \quad (4.4)$$

where $\overline{R}$ is the average value of R and is stated as:

$$\bar{R}(L^*-L,N^*-N) = \frac{[\,(L^*-L+0.5)^2-(N^*-N-0.5)^2\,]^{0.5}}{(L^*-L+0.5)(N^*-N-0.5)} - \frac{[\,(L^*-L+0.5)^2-(N^*-N+0.5)^2]^{0.5}}{(L^*-L+0.5)(N^*-N+0.5)} \quad (4.5)$$

In that equation (4.4), $A(L,N), B(L,N),\ and\ C(L,N)$ are defined as geometry factors. They determine which element will or will not remain within the wing geometry and enable weight factors to be determined based on the position of the panels (Bertin, 2008).

$A(L,N)$ determines the wing leading edge geometry and takes values in the range $[0,1]$. If the panel is in front of the leading edge, $A(L,N)$ takes the value 0. If the panel is behind the leading edge but is too close to it, the $A(L,N)$ takes the distance value between the panel and the leading edge. If the panel is far behind the leading edge, A takes the value 1. All this can be summarized as follows.

$$A(L,N) = 0 \qquad L - x_{LE} \leq 0$$
$$A(L,N) = L - x_{LE} \qquad 0 < L - x_{LE} < 1$$
$$A(L,N) = 1 \qquad L - x_{LE} \geq 1$$

$B(L,N)$ determines the wing trailing edge geometry and takes values in the range $[0,1]$. If the panel is behind trailing edge, it takes the value 0. If the panel is in front of the trailing edge and far enough away, it takes the value 1. All this can be summarized as follows.

$$B(L,N) = 0 \qquad L - x_{TE} \geq 1$$
$$B(L,N) = 1 - (L - x_{TE}) \qquad 0 < L - x_{TE} < 1$$
$$B(L,N) = 1 \qquad L - x_{TE} \leq 0$$

$C(L,N)$ is for the wing tip weighting factor taking values of 0.5 or 1. If the panel is at the wing tip, $C(L,N)$ takes the value 0.5. It takes the value 1 for all other cases.

$$C(L,N) = 0.5 \qquad N = N_{max}$$
$$C(L,N) = 1 \qquad N \neq N_{max}$$

When the above mentioned calculations are performed in a suitable order, the differential pressure coefficient $\Delta C_p(L^*,N^*)$ can easily be found at a field point on a arbitrary wing or a lifting surface.

Some issues to be considered and not to be forgotten while making the calculations are as follows:

- While calculating $\Delta C_p(L^*,N^*)$, it should be started from the wing apex point and a backward sequence should be followed (increasing values of L^*). When this order is followed, since all the points in the Mach cone arising from the field point (L^*,N^*) will be calculated, there will be no unknown value in the summation in the equation (4.4) (Bertin, Cumming,2013).

- Each panel can only be affected by the panels inside the Mach cone in front of it. Since the influence function in equation (4.5) will take the value 0, it can be said that a panel has no effect on itself, and zero value must be taken directly (Carlson and Miller,1974).

When performing numerical analysis, a smooth process is required that can eliminate large fluctuations in pressure coefficient. Consequently, the algorithm taken from the study by Carlson and Miller (1974) is directly as follows (Bertin, Cumming,2013):

1. Calculate and retain, temporarily, the preliminary ΔC_p values for a given row, with $L^* = constant$. Designate this as $\Delta C_{p,a}(L^*,N^*)$.

2. Calculate and retain, temporarily, ΔC_pvalues for the following row with $L^* = constant + 1$, by using the $\Delta C_{p,a}$ values obtained in the previous step for contributions from the row with $L^* = constant$. Designate this as $\Delta C_{p,b}(L^*,N^*)$.

3. Calculate a final ΔC_p value from a fairing of integrated preliminary ΔC_p results.

   For leading-edge elements, defined as $L^* - x_{LE}(N^*) \leq 1$,

$$\Delta C_p(L^*,N^*) = \frac{1}{2}\left[1 + \frac{A(L^*,N^*)}{1 + A(L^*,N^*)}\right]\Delta C_{p,a}(L^*,N^*) + \frac{1}{2}\left[\frac{A(L^*,N^*)}{1 + A(L^*,N^*)}\right]\Delta C_{p,b}(L^*,N^*)$$

For all other elements defined as $L^* - x_{LE}(N^*) > 1$,

$$\Delta C_p(L^*,N^*) = \frac{3}{4}\Delta C_{p,a}(L^*,N^*) + \frac{1}{4}\Delta C_{p,b}(L^*,N^*)$$

4.3 Aerodynamic Coefficients

After calculating the differential pressure coefficient for all panels, the aerodynamic coefficients like $C_L, C_M, and\ C_D$ for wing surface can be calculated as following respectively:

The Lift Coefficient:

$$C_L = \frac{2}{\beta S} \sum_{N^*=0}^{N^*=N_{max}} \sum_{L^*=L_{LE}}^{L^*=L_{TE}} \left[\frac{3}{4} \Delta C_p(L^*, N^*) + \frac{1}{4} \Delta C_p(L^*+1, N^*) \right] A(L^*, N^*) B(L^*, N^*) C(L^*, N^*)$$

The Pitching-Moment Coefficient:

$$C_M = \frac{2}{\beta S \bar{c}} \sum_{N^*=0}^{N^*=N_{max}} \sum_{L^*=L_{LE}}^{L^*=L_{TE}} (L^*) \left[\frac{3}{4} \Delta C_p(L^*, N^*) + \frac{1}{4} \Delta C_p(L^*+1, N^*) \right] A(L^*, N^*) B(L^*, N^*) C(L^*, N^*)$$

The Drag Coefficient:

$$C_D = -\frac{2}{\beta S} \sum_{N^*=0}^{N^*=N_{max}} \sum_{L^*=L_{LE}}^{L^*=L_{TE}} \left[\frac{3}{4} \Delta C_p(L^*, N^*) + \frac{1}{4} \Delta C_p(L^*+1, N^*) \right] \left[\frac{3}{4} \frac{\partial z_c(L^*, N^*)}{\partial x} + \frac{1}{4} \frac{\partial z_c(L^*+1, N^*)}{\partial x} \right] A(L^*, N^*) B(L^*, N^*) C(L^*, N^*)$$

The wing area S used in the above equations can be obtained as

$$S = \frac{2}{S} \sum_{N^*=0}^{N^*=N_{max}} \sum_{L^*=1+x_{LE}}^{L^*=1+x_{TE}} A(L^*, N^*) B(L^*, N^*) C(L^*, N^*)$$

5. DEVELOPED MODULE and VALIDATION

In this section, the code written using Matlab for different wing types will be introduced and the code results for validation will be compared with the literature information.

5.1 Developed Code

5.2 Validation Studies

5.2.1 Delta wing

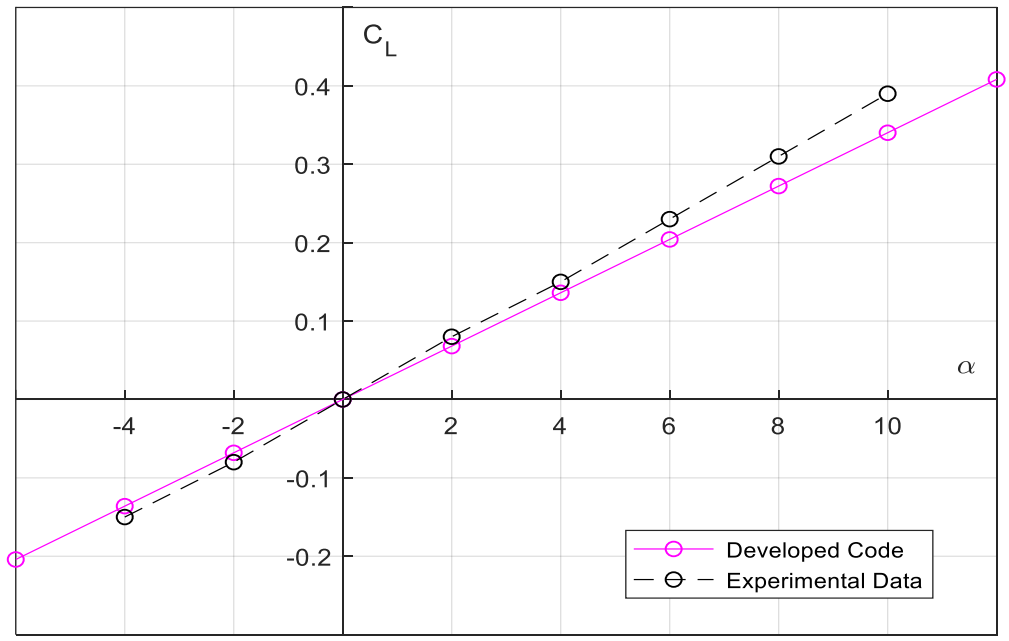

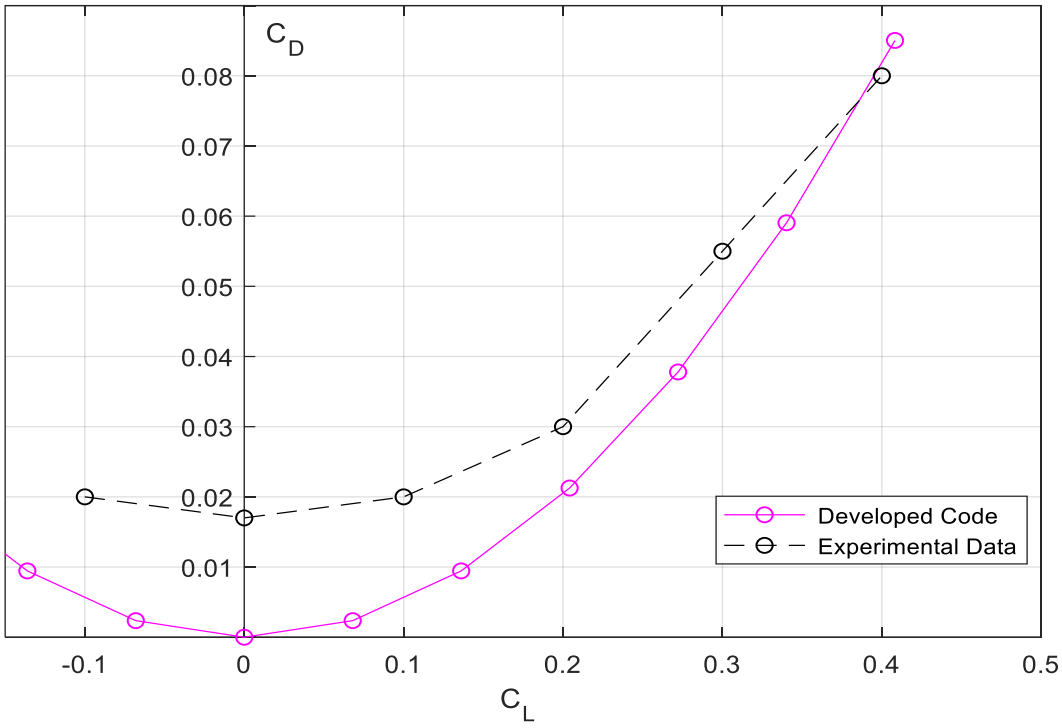

5.2.2 Trapez wing

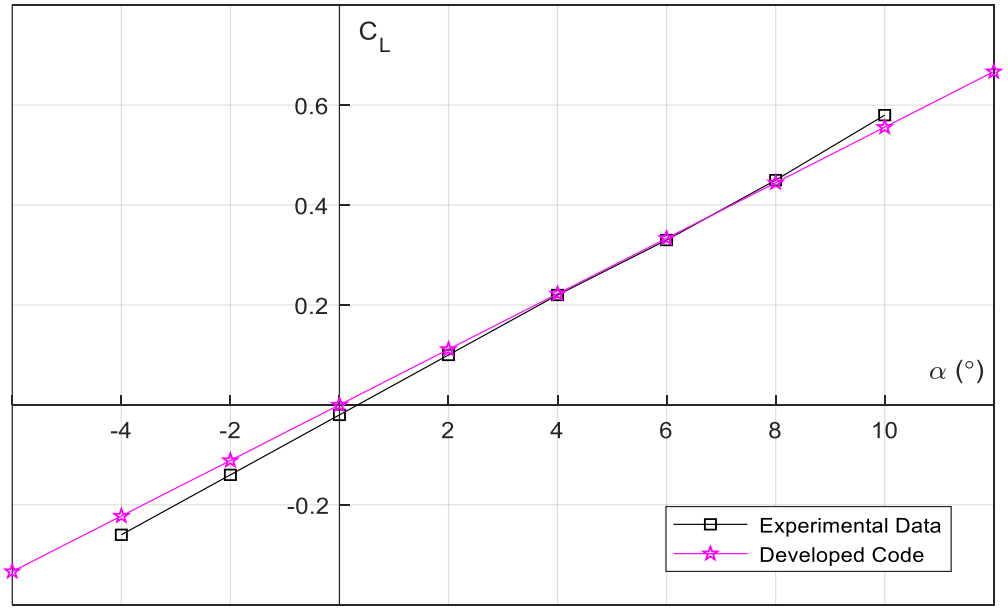

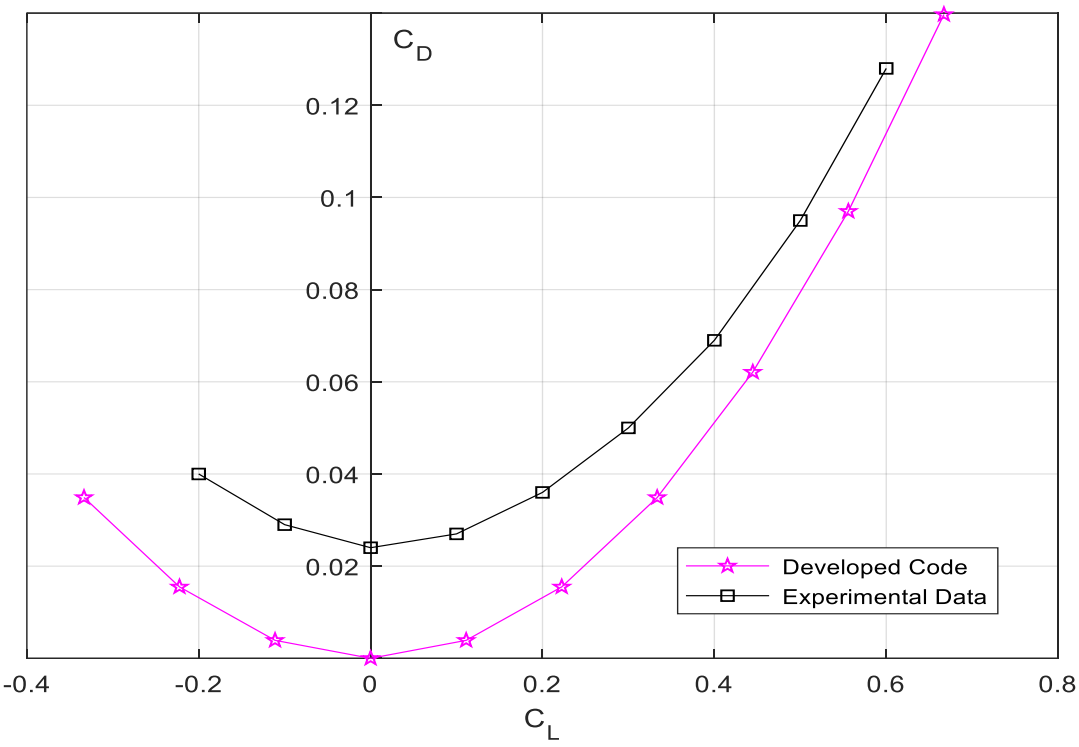

5.2.3 Arrow wing

5.2.4 Double-delta wing

6. CONCLUSIONS

REFERENCES

APPENDICES

APPENDIX A

```
clc
clear all
wing = menu('Choose a wing configuration',...
 'Delta','Double Delta','Arrow','Trapez');

if wing == 1
 choice = inputdlg({'Mach Number','Angle of Attack',...
 'Sweep Angle (DEG)'},...
 'Flow and Wing Characteristics',...
 [1 60; 1 60; 1 60]);

elseif wing == 2
 choice = inputdlg({'Mach Number','Angle of Attack',...
 '1st Sweep Angle (DEG)','2nd Sweep Angle (DEG)'},...
 'Flow and Wing Characteristics',...
 [1 60; 1 60; 1 60; 1 60]);

elseif wing == 3
 choice = inputdlg({'Mach Number','Angle of Attack',...
 'LE Sweep Angle (DEG)','TE Sweep Angle (DEG)'},...
 'Flow and Wing Characteristics',...
 [1 60; 1 60; 1 60; 1 60]);

elseif wing == 4
 choice = inputdlg({'Mach Number','Angle of Attack',...
 'LE Sweep Angle (DEG)','TE Sweep Angle (DEG)'},...
 'Flow and Wing Characteristics',...
 [1 60; 1 60; 1 60; 1 60]);
end
M = str2num(choice{1});
beta = sqrt(M^2-1);
alfa_deg = str2num(choice{2});
alfa_rad = alfa_deg*(pi/180);
if wing == 1
 sweep = acotd(cotd(str2num(choice{3}))/beta);
 L = 1:80;
 N = -50:50;

elseif wing == 2
 sweep1 = acotd(cotd(str2num(choice{3}))/beta);
 sweep2 = acotd(cotd(str2num(choice{4}))/beta);
 L = 1:20;
 N = -10:10;

else
 le_sweep = acotd(cotd(str2num(choice{3}))/beta);
```

```
 te_sweep = acotd(cotd(str2num(choice{4}))/beta);
 L = 1:80;
 N = -50:50;
end

for i = 1:max(L)
 for j = 0:max(N)

 if wing == 1
 x_le(j+1) = j/cotd(sweep);
 x_te(j+1) = max(N)/cotd(sweep);

 elseif wing == 2
 if j <= round(max(N)/3.4)
 x_le(j+1) = j/cotd(sweep1);
 else
 x_le(j+1) = x_le(round(max(N)/3.4))+ j/cotd(sweep2);
 end
 x_te(j+1) = max(L);

 elseif wing == 3
 x_le(j+1) = j/(beta*cotd(le_sweep));
 if j == 0
 x_te(j+1) = max(L)-max(N)/cotd(te_sweep);
 else
 x_te(j+1) = x_te(1) + j/cotd(te_sweep);
 end

 elseif wing == 4
 x_le(j+1) = j/cotd(le_sweep);
 if j == 0
 x_te(j+1) = max(L);
 else
 x_te(j+1) = max(L)- j/cotd(te_sweep);
 end
 end

 if L(i)-x_le(j+1) <= 0
 A(i,j+1) = 0;
 elseif L(i)-x_le(j+1) >= 1
 A(i,j+1) = 1;
 else
 A(i,j+1) = L(i)-x_le(j+1);
 end

 if L(i)-x_te(j+1) >= 1
 B(i,j+1) = 0;
 elseif L(i)-x_te(j+1) <= 0
 B(i,j+1) = 1;
 else
```

```
 B(i,j+1) = 1-(L(i)-x_te(j+1));
 end

 C = ones(max(L),max(N)+1);
 C(max(L),max(N)+1) = 0.5;

 end
end

A = [fliplr(A) A(:,2:end)];
B = [fliplr(B) B(:,2:end)];
C = [fliplr(C) C(:,2:end)];
x_le = [flip(x_le) x_le(2:end)];
x_te = [flip(x_te) x_te(2:end)];
Cp = zeros(length(L),length(N));
Cp_b = zeros(length(L),length(N));
for i = 1:max(L)
for j = max(N):(length(N)-1)
 if and((L(i)-x_le(j+1))>=0, round(L(i)-x_te(j+1))<=0)
 R_a = zeros(length(L),length(N));
 for m = 1:(i-1)
 for n = 1:length(N)
 if and(abs(atand((N(n)-N(j+1))/(L(m)-L(i))))<=45 ,...
 L(m)-x_le(n)>=0)
 R_a(m,n) = ((L(i)-L(m)+0.5)^2-...
 (N(j+1)-N(n)-0.5)^2)^0.5...
 /((L(i)-L(m)+0.5)*(N(j+1)-N(n)...
 -0.5))-((L(i)-L(m)+0.5)^2-...
 (N(j+1)-N(n)+0.5)^2)^0.5/((L(i)-...
 L(m)+0.5)*(N(j+1)-N(n)+0.5));

 else
 R_a(m,n) = 0;
 end
 end
 end
 Cp(i,j+1) = 4/beta*alfa_rad+1/pi*sum(sum(R_a.*A.*B.*C.*Cp));
 Cp = [ fliplr(Cp(:,(max(N)+2):end)) Cp(:,(max(N)+1):end)];

 else
 Cp(i,j+1) = 0;
 end
 end
for j = max(N):(length(N)-1)

 if i ~= length(L)
 R_b = zeros(length(L),length(N));
 for m = 1:i
 for n = 1:length(N)
 if and(abs(atand((N(n)-N(j+1))/(L(m)-L(i+1))))<=45 ,...
```

```
 L(m)-x_le(n)>0)

 R_b(m,n) = ((L(i+1)-L(m)+0.5)^2-(N(j+1)-N(n)...
 -0.5)^2)^0.5/((L(i+1)-L(m)+0.5)*...
 (N(j+1)-N(n)-0.5))-((L(i+1)-L(m)+0.5)^2-...
 (N(j+1)-N(n)+0.5)^2)^0.5/...
 ((L(i+1)-L(m)+0.5)*(N(j+1)-N(n)+0.5));
 else
 R_b(m,n) = 0;

end
 end
 end
 else
 R_b(i,j+1) = 0;

 end

 if or(L(i)-x_le(j+1)<0 , round(L(i)-x_te(j+1))>0)
 Cp_b(i,j+1) = 0;
 else
 Cp_b(i,j+1) = 4/beta*alfa_rad+1/pi*sum(sum(R_b.*A.*B.*C.*Cp));
 Cp_b = [ fliplr(Cp_b(:,(max(N)+2):end)) Cp_b(:,(max(N)+1):end)];
 end
end
for j = max(N):(length(N)-1)

 if L(i)-x_le(j+1)<=1
 Cp(i,j+1) = (1/2)*(1+A(i,j+1)/(1+A(i,j+1)))*Cp(i,j+1)+(1/2)*...
 (A(i,j+1)/(1+A(i,j+1)))*Cp_b(i,j+1);
 else
 Cp(i,j+1) = (3/4)*Cp(i,j+1)+(1/4)*Cp_b(i,j+1);
 end

 Cp = [ fliplr(Cp(:,(max(N)+2):end)) Cp(:,(max(N)+1):end)];

end
end
%Wing Area
S = (2/beta)*sum(sum(A.*B.*C));
%Wing Span
b = length(N);
%Wing Mean Chord
c = S/b;
%Wing Slope
slope = zeros(max(L),length(N));
slope(:,:) = -alfa_rad;
slope_L = [ slope(2:end,:) ; zeros(1,length(N))];
%Cp(L+1,N)
Cp_L = [ Cp(2:end,:) ; zeros(1,length(N))];
```

```
%AERODYNAMIC COEFFICIENTS FOR THE WING
%Lift Coefficient
C_L = (2/(beta*S))*sum(sum(((3/4)*Cp+(1/4)*Cp_L).*A.*B.*C));
%Pitching-moment Coefficient
C_M = (2/(beta*S*c))*sum(sum(transpose(L).*((3/4)*Cp+(1/4)*Cp_L).*...

A.*B.*C));

%Drag Coefficient C_D = -(2/(beta*S))*sum(sum(((3/4)*Cp+(1/4)*Cp_L).*...
((3/4)*slope+(1/4)*slope_L).*A.*B.*C));
```